



## Micrometeorological fluxes under the influence of regional and local advection: a revisit

Xuhui Lee<sup>a,\*</sup>, Qiang Yu<sup>b</sup>, Xiaomin Sun<sup>b</sup>, Jiandong Liu<sup>c</sup>,  
Qingwen Min<sup>b</sup>, Yunfen Liu<sup>b</sup>, Xianzhou Zhang<sup>b</sup>

<sup>a</sup> School of Forestry and Environmental Studies, Yale University, 370 Prospect Street, New Haven, CT 06511, USA

<sup>b</sup> Institute of Geographic Sciences and Natural Resources Research, Chinese Academy of Sciences, Beijing, China

<sup>c</sup> Center for Agrometeorology, Chinese Academy of Meteorological Sciences, Beijing, China

Received 13 June 2001; received in revised form 9 September 2002; accepted 24 February 2003

### Abstract

This paper presents a new analysis of inequality of eddy diffusivities for sensible heat ( $K_H$ ) and water vapor ( $K_W$ ). It is shown that the same set of equations, established on the principle of dual-source diffusion, can be applied to both local and regional advection. Various advection scenarios are discussed using a formula that relates  $K_H/K_W$  to the Bowen ratio of the advective source and the observed gradient Bowen ratio ( $\beta_g$ ) near the ground surface. A similar analysis can also be performed for eddy diffusivities for trace gases.

The ratio  $K_H/K_W$ , observed at a well-watered wheat field in the North China Plains, was mostly greater than unity when  $\beta_g$  was negative and smaller than unity when  $\beta_g$  was positive. The pattern was consistent with the theoretical analysis of the ratio under the influence of regional advection. Some degree of local advection was also suggested by the data. Despite inequality of the eddy diffusivities, there was little systematic bias between the evapotranspiration rates measured with a Bowen ratio/energy balance and an eddy covariance system.

© 2003 Elsevier B.V. All rights reserved.

**Keywords:** Advection; Inversion; Evapotranspiration; Bowen ratio

### 1. Introduction

Wheat is a top cereal crop in China. It is known that water availability is a primary factor in influencing its grain yield (Jones, 1992), and wheat-growing farmers in China irrigate their fields, wherever possible, in order to improve yield. Accurate measurement of evaporative water loss is needed for strategic planning of irrigation water. While the eddy covariance

(EC) is widely used in micrometeorological research in the Western countries, the Bowen ratio/energy balance (BREB) method of measuring evapotranspiration (ET) remains an attractive approach in China and other developing countries because of its low cost and long-term reliability.

BREB is also a useful tool in studies of micrometeorological fluxes of trace gases such as CO<sub>2</sub> (Dugas et al., 1999; Leuning et al., 1998; Price and Black, 1991), hydrocarbon (Godlstein et al., 1996), and atmospheric mercury (Meyers et al., 1996). In these studies, the BREB measurement is used to derive the eddy diffusivity for water vapor ( $K_W$ ), which

\* Corresponding author. Tel.: +1-203-432-6271;

fax: +1-203-432-3929.

E-mail address: [xuhui.lee@yale.edu](mailto:xuhui.lee@yale.edu) (X. Lee).

is then used in the computation of the trace gas fluxes.

The BREB approach assumes equality of eddy diffusivities for heat ( $K_H$ ), water vapor and other scalars of interest. It is known that latent heat flux from well-watered crops can exceed net radiation, with the excess energy provided by advection of sensible heat from adjacent dry fields. The validity of the equality assumption under such advection conditions has been investigated experimentally by a number of researchers (Blad and Rosenberg, 1974; Motha et al., 1979; Verma et al., 1978). They showed that  $K_H$  exceeded  $K_W$  by various amounts and concluded that the equality assumption could result in consistent underestimation of ET. Their conclusion is supported by a more recent, carefully conducted study (Laubach et al., 2000). On the other hand, Lang et al. (1983) showed a case of  $K_H < K_W$  and argued that their result was consistent with the theory of Launder (1978).

In the North China Plains, farmers grow winter wheat as the only cereal crop from October to May. Because climate in the growing season is dry (precipitation often less than 100 mm), irrigation is widespread, creating a moist lower atmospheric boundary layer in an otherwise dry climate. Regional advection<sup>1</sup> is expected to play a role in the surface-layer exchange processes. Some influence of local advection may also arise from the spatial heterogeneity in soil water status caused by differences in the timing and amount of irrigation in adjacent farms, but unlike previous studies on advection which focus almost exclusively on sharp dry-to-wet transitions, local advection there is less pronounced.

This paper revisits the issue of inequality of eddy diffusivities under the influence of advection using a dataset obtained over an irrigated wheat field in the North China Plains. In the experiment, we observed departures between  $K_H$  and  $K_W$  that were much larger than reported in the literature. We also found that depending on the stability of the surface layer,  $K_H$  could be either greater or smaller than  $K_W$ . In order to explain these seemingly unusual results, in Section 2

we present a theoretical analysis of how the eddy diffusivities should behave in various advection scenarios by decomposing the eddy diffusion according to source characteristics, following McNaughton and Laubach (1998), Moeng and Wyngaard (1984) and others. In our analysis, we seek an explanation that can be applied to both local advection and regional advection. A brief description of the micrometeorological experiment in the North China Plains is given in Section 3. In Section 4, the experimental results are presented and are compared with the theoretical prediction.

## 2. Theory

### 2.1. Diffusion from dual sources

It has been long recognized that in situations where diffusion is affected by dual sources, eddy diffusivity in the simple gradient-diffusion equation often behaves differently from that of a single source diffusion (e.g., Deardorff, 1978; Denmead and Bradley, 1985; Wyngaard and Brost, 1984). The present development follows the lines suggested by McNaughton and Laubach (1998). Let us suppose that the heat and water vapor fluxes originated from the underlying surface are marked by a red tracer whose diffusivity is  $K_R$ , and those originated elsewhere are marked by a yellow tracer with a diffusivity  $K_Y$ . In the case of local advection where the internal boundary layer is not fully adjusted to the red source, the yellow heat and water vapor come from an upwind area. In a fully adjusted internal boundary layer, the yellow scalars are originated from the top of the boundary layer.

On the principle of linear superposition, the total flux of sensible heat,  $H$ , and potential temperature,  $\theta$ , are decomposed as

$$H = H_Y + H_R, \quad (1)$$

$$\theta = \theta_Y + \theta_R. \quad (2)$$

Substituting the following flux–gradient relationships

$$\begin{aligned} H &= -K_H \frac{\partial \theta}{\partial z}, & H_Y &= -K_Y \frac{\partial \theta_Y}{\partial z}, \\ H_R &= -K_R \frac{\partial \theta_R}{\partial z}, \end{aligned} \quad (3)$$

<sup>1</sup> An operational definition of regional advection is given by Rosenberg et al. (1983) who consider the observation to be influenced by regional advection (of sensible heat) if sensible heat flux is of opposite sign to the net radiation flux. Obviously, some degree of regional advection can also exist at times of positive sensible heat flux.

into Eq. (1) and making use of Eq. (2), we obtain

$$K_H = \alpha_\theta K_Y + (1 - \alpha_\theta) K_R, \quad (4)$$

where  $\alpha_\theta = (\partial\theta_Y/\partial z)/(\partial\theta/\partial z)$ . A similar equation can be written for the eddy diffusivity for total water vapor,  $K_W$ , as

$$K_W = \alpha_q K_Y + (1 - \alpha_q) K_R, \quad (5)$$

where  $\alpha_q = (\partial q_Y/\partial z)/(\partial q/\partial z)$ , with  $q$  denoting humidity. Manipulation of Eqs. (4) and (5) yields

$$\frac{K_H}{K_W} = 1 - \frac{(1 - K_R/K_Y)(1 - \beta_Y/\beta_g)}{1 + (1/\alpha_q - 1)K_R/K_Y}, \quad (6)$$

where  $\beta_Y$  is the Bowen ratio of the yellow source, and  $\beta_g$  the gradient Bowen ratio for the total heat and water vapor. Note that the flux and gradient Bowen ratios of the yellow source are identical and that  $\beta_g$  is related to the overall flux Bowen ratio,  $\beta_f = H/\lambda E$ , as

$$\beta_f = \frac{K_H}{K_W} \beta_g, \quad (7)$$

where  $\lambda$  is latent heat of vaporization and  $E$  the overall water vapor flux.

We wish to make two points regarding Eq. (6) before embarking on a discussion of various advection scenarios. First, while  $K_R$  follows the surface-layer similarity theory, the exact form of  $K_Y$  is not known. However, it is assumed that  $K_Y$  is greater than  $K_R$  because large eddies generated in the boundary layer influence the yellow scalars more than the red scalars (McNaughton and Laubach, 1998; Wyngaard and Brost, 1984). It follows that the denominator of the second term on the RHS of Eq. (6) is positive. Second,  $\beta_Y$  is a conserved property that does not change as the yellow scalars advect downwind (in the case of local advection) or as they diffuse downward from the upper boundary layer (in the case of regional advection). This is because turbulent eddies are not discriminative in transporting the scalars they have picked up at the same source location.

## 2.2. Local advection

Let us consider the situation of an abrupt change of the surface source, from yellow to red, with the experiment performed downwind of the transition. If the measurement is made too far above the ground where the internal boundary layer is not fully adjusted to the

red source, both the upwind yellow source and the underlying red source will contribute to the observed gradients. Horizontal advection is not negligible so that the sum of the vertical sensible and latent heat fluxes needs not to be in balance with the available energy. Numerous possibilities exist that can lead to inequality of the eddy diffusivities, but two scenarios are the most obvious, which are presented further.

### 2.2.1. Wet-to-dry transition

In this scenario, the red source is assumed to be relatively dry so that the observed gradient Bowen ratio,  $\beta_g$ , is positive (lapse temperature profile over the red source). Because the yellow source is wet,  $\beta_Y$  is smaller than  $\beta_g$ . According to Eq. (6), the eddy diffusivity for sensible heat,  $K_H$ , is smaller than that for water vapor,  $K_W$ . The eddy diffusivities ratio can even become negative (counter-gradient transport of sensible heat) if  $\beta_Y$  is negative (i.e., inversion over the yellow source) and  $\beta_g$  takes a value close to zero (i.e., air over the red source being near neutral). An illustrative calculation of the eddy diffusivities ratio is presented in Fig. 1 (solid line).

### 2.2.2. Dry-to-wet transition

In this scenario, the Bowen ratio of the dry yellow source,  $\beta_Y$ , is assumed positive (lapse temperature profile over the yellow source) and is normally greater than  $\beta_g$ . The sign of  $\beta_g$  determines whether or not  $K_H$  exceeds  $K_W$ . If a lapse temperature profile prevails over the red source (positive  $\beta_g$ ), the ratio  $\beta_Y/\beta_g$  exceeds unity and  $K_H$  is greater than  $K_W$ . If, on the other hand, a surface inversion exists over the red source (negative  $\beta_g$ ), the ratio  $\beta_Y/\beta_g$  is negative, and  $K_H$  is once again smaller than  $K_W$  (Fig. 1, dashed line). The observation of Lang et al. (1983) could be considered an example of local advection from dry to wet surface, in an internal boundary layer that was not in full equilibrium with the wet surface. If the yellow source is extremely dry,  $\beta_Y$  should approach infinity and the humidity parameter  $\alpha_q$  should approach zero. It can be shown that in this limit, Eq. (6) reduces to the special case studied by McNaughton and Laubach (1998).

## 2.3. Regional advection

At a downwind location of large distance from the leading edge, the sufficiently deepened internal

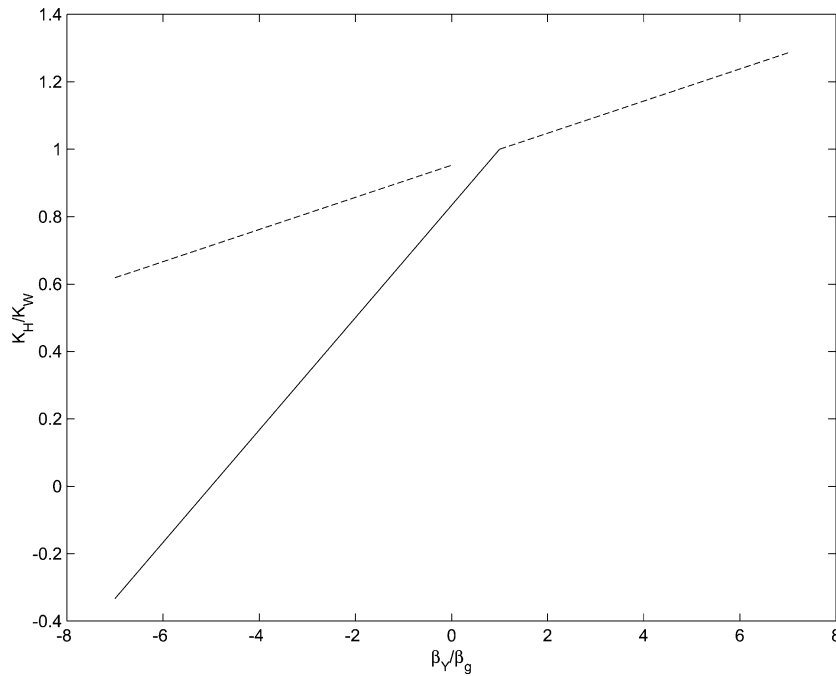


Fig. 1. Ratio of the eddy diffusivities plotted against the ratio of the Bowen ratio of the upwind source to the total gradient Bowen ratio ( $\beta_Y/\beta_g$ ): solid line, wet-to-dry transition ( $\beta_g > 0$ ); dashed line, dry-to-wet transition ( $\beta_Y > 0$ ). Calculations are made with  $K_R/K_Y = 0.8$ ,  $\alpha_q = 0.8$  for the wet-to-dry transition and 0.2 for the dry-to-wet transition.

boundary layer resembles that of a typical daytime atmospheric boundary layer over land, with the surface layer and the elevated inversion layer separated by a mixed layer (Fig. 2). Because the surface sensible heat flux is small in magnitude, the mixed layer is usually shallower than found over dry land. The scalars released by the source upwind are now well mixed and exert no direct influence on the vertical gradients in the surface layer. Horizontal advection is negligible within the surface layer. However, the

surface layer diffusion is “contaminated” by scalars transported downward from the elevated inversion by large eddies. It is appropriate to label this type of heat transport as regional advection because top-down diffusion of heat occurs at a regional scale.

The same set of relationships discussed in Section 2.1 holds if we now tag the source at the elevated inversion with a yellow tracer and the ground-level source with a red tracer, noting that the Bowen ratio of the yellow source is usually negative. Two

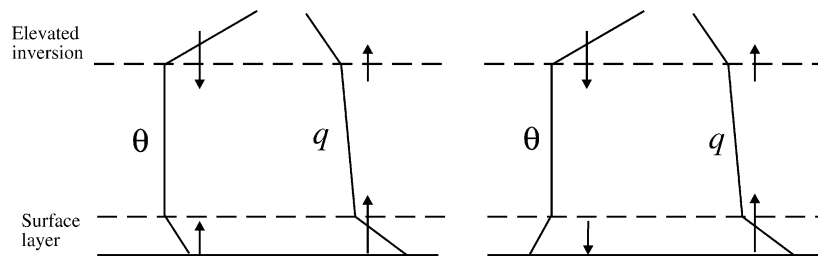


Fig. 2. A schematic diagram of a fully developed internal boundary layer over a moist surface: left, unstable surface layer; right, ground-level inversion. Regional advection occurs in the form of downward diffusion of sensible heat from the elevated inversion. Arrows indicate directions of fluxes.

scenarios can be constructed. In scenario 1, the surface layer is slightly unstable ( $\beta_g > 0$ ), and Eq. (6) predicts that  $K_H < K_W$ .

In scenario 2, an inversion exists at the ground and hence  $\beta_g < 0$ . The diffusivities ratio is determined by the relative magnitudes of  $\beta_Y$  and  $\beta_g$ . Experimental results suggest that  $\beta_g$  is typically greater than  $-0.5$  under the influence of regional advection (Verma et al., 1978; Laubach et al., 2000; see also Fig. 5). The magnitude of  $\beta_Y$  is less certain. The analysis of heat and water vapor budgets of the convective boundary layer over the FIFE and BOREAS sites shows that the Bowen ratio of the entrainment fluxes at the boundary layer top fall in the range from  $-2$  to  $-0.3$  (Barr and Betts, 1997; Betts et al., 1992). No data of this kind are available for the internal boundary layer over an extensive and moist surface, but one can proceed by examining the relative magnitudes of the surface fluxes and fluxes at the elevated inversion. Typically in daylight hours, the humidity of the internal boundary layer increases with time; this requires that the upward entrainment flux of water vapor at the elevated inversion be smaller than the surface flux value. On

the other hand, because air above the internal boundary layer is much warmer than below, the downward sensible heat flux at the elevated inversion must be larger in magnitude than the flux to the ground surface. This large sensible heat flux is necessary to sustain an important element of regional advection, that is, the daytime continuous warming and growth of the internal boundary layer despite the negative sensible heat flux at the ground level. For example, Verma et al. (1978) reported a temperature increase of  $5^\circ\text{C}$  from 10:00 to 19:00 local time over an air layer up to 16 m above the ground. Also their vertical temperature gradient became progressively larger with time, suggesting the deepening of the internal boundary layer. In the present study, air was much warmer in the late afternoon than in the early morning, with a temperature increase of  $10\text{--}15^\circ\text{C}$ . We therefore argue that in the presence of regional advection,  $\beta_Y$  should be more negative than  $\beta_g$ . Thus, in scenario 2, the ratio  $K_H/K_W$  exceeds unity.

By holding other parameters in Eq. (6) at constant values ( $\beta_Y = -1$ ,  $\alpha_q = 0.2$ ,  $K_R/K_Y = 0.8$ ), Fig. 3 shows how the eddy diffusivities ratio varies

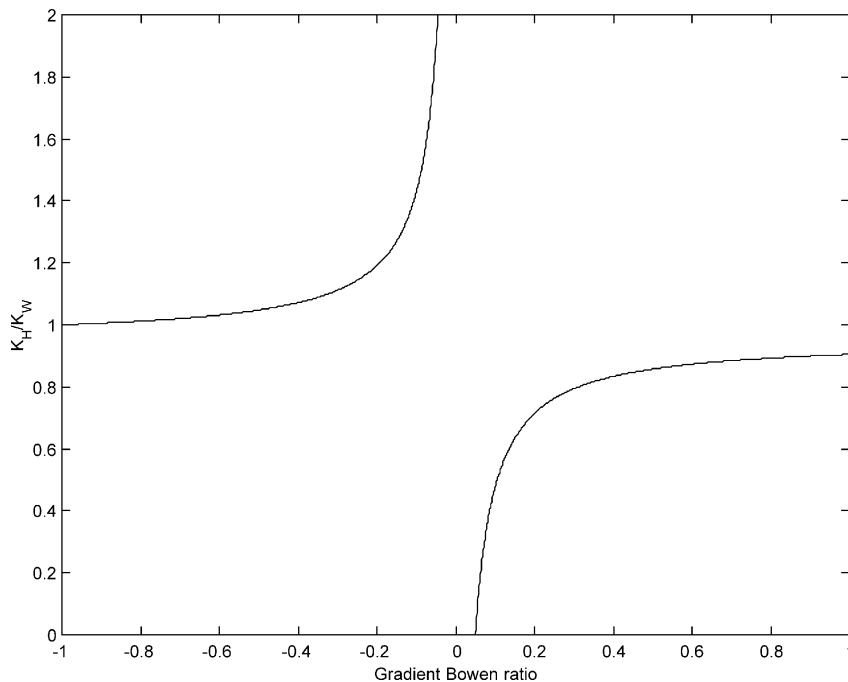


Fig. 3. Ratio of eddy diffusivities as a function of the gradient Bowen ratio ( $\beta_g$ ) in the surface layer under the influence of regional advection. Calculations are made with  $K_R/K_Y = 0.8$ ,  $\alpha_q = 0.2$  and  $\beta_Y = -1$ .

as a function of  $\beta_g$ . Our result is in broad agreement with McNaughton and Laubach (1998) who seek to explain inequality of the eddy diffusivities on the ground of a two-scale Reynolds decomposition of the wind and scalar variables into active and inactive components.

#### 2.4. Discussion

Eq. (6) is a convenient diagnostic tool for discovering situations in which equality of the eddy diffusivities is not satisfied. However, the strictly formal analysis cannot be used to make a quantitative prediction because of the unknown diffusivity  $K_Y$ . It also ignores the feedback between the surface ET, saturation deficit, and depth of the boundary layer (Brunet et al., 1994; Kroon and de Bruin, 1995; Zermeno and Hippias, 1997; McNaughton and Spriggs, 1989), and the fact that sensible and latent heat fluxes are constrained by the available energy. Accordingly,  $\alpha_q$ ,  $\beta_Y$  and  $\beta_g$  cannot be treated as independent variables as in the illustrative calculations shown in Figs. 1 and 3. Despite this shortcoming, Eq. (6) clearly highlights the inadequacy of the equality assumption in advective conditions.

A question that arises naturally from the above analysis is whether the equality assumption holds in convective boundary layer over dry land because the transport of sensible heat and water vapor is also a dual-source process. The large eddy simulation of Moeng and Wyngaard (1984) shows that the humidity gradient due to top-down diffusion,  $\partial q_Y / \partial z$ , is vanishingly small in the surface layer, or  $1/\alpha_q \rightarrow \infty$ , because this layer is separated from the inversion layer by a deep mixed layer. Furthermore, if local advection is absent, Eq. (6) reduces to the equality relation,  $K_H/K_W = 1$ . However, the top-down diffusion may be non-negligible at times (e.g., morning transitional period) when the mixed layer is shallow.

A similar analysis can be also performed for  $\text{CO}_2$  in advective flow. Let us suppose that the measurement is made over a surface which is a sink of  $\text{CO}_2$ , at a location downwind of a source of  $\text{CO}_2$  where the internal boundary layer is not fully equilibrated with the surface. The situation is analogous to the dry-to-wet transition discussed in Section 2.2. It can be shown that the diffusivity for  $\text{CO}_2$  is smaller than that for water vapor.

### 3. Experimental methods

#### 3.1. Site

The experiment was conducted at the Yucheng Agricultural Experiment Station, Chinese Academy of Sciences, in Yucheng, 350 km south of Beijing ( $36^\circ 57' \text{N}$ ,  $116^\circ 36' \text{E}$ ). The measurement was made at the center of a  $300 \text{ m} \times 300 \text{ m}$ , well-watered field of winter wheat. At the time of the experiment, the leaf area index was in the range 4.3–6.6 (Table 1). Surrounding the experimental field was unbroken farmland of winter wheat, at similar growth stages and also with ample water supply, that extended at least 5 km in all direction. Except for the southeast wind direction where our laboratory buildings may have interfered with the flow, the effective aerodynamic fetch was much greater than the dimension of the experimental farm.

#### 3.2. Instrumentation

The key instrumentation included a commercial EC system and a homemade BREB system. The EC system consisted of a 3D sonic anemometer (model DA600, Kajio, Japan, 20 cm pathlength) and an open-path  $\text{H}_2\text{O}/\text{CO}_2$  analyzer (model E009, Advanet Inc., Okayama, Japan, 20 cm pathlength) and was mounted at 2 m above the canopy. The two sensors were separated by 30 cm along the predominant wind direction. The EC signals were sampled at 20 Hz and eddy fluxes were computed over 10 min intervals. Correction for density effects was applied to the water vapor flux.

The BREB system consisted of a net radiometer (manufactured and calibrated by Jinzhou 322,

Table 1

Background meteorological conditions during the experiment (day-time mean values): wind speed ( $u$ ,  $\text{m s}^{-1}$ ), relative humidity ( $r$ , %), fluxes of sensible heat ( $H$ ,  $\text{W m}^{-2}$ ), latent heat ( $\lambda E$ ,  $\text{W m}^{-2}$ ) and net radiation ( $R_n$ ,  $\text{W m}^{-2}$ ), heat flux into the soil ( $G$ ,  $\text{W m}^{-2}$ ), and the Priestley–Taylor parameter ( $\alpha$ , Eq. (8))

Date	LAI	$u$	$r$	$H$	$\lambda E$	$R_n$	$G$	$\alpha$
26 April	6.6	–	60	–21	303	282	10	1.60
27 April		–	63	–25	252	252	11	1.62
17 May	4.3	3.0	63	–2	290	378	10	1.40
18 May		1.5	64	32	323	361	11	1.26
19 May		2.1	51	45	312	409	8	1.28

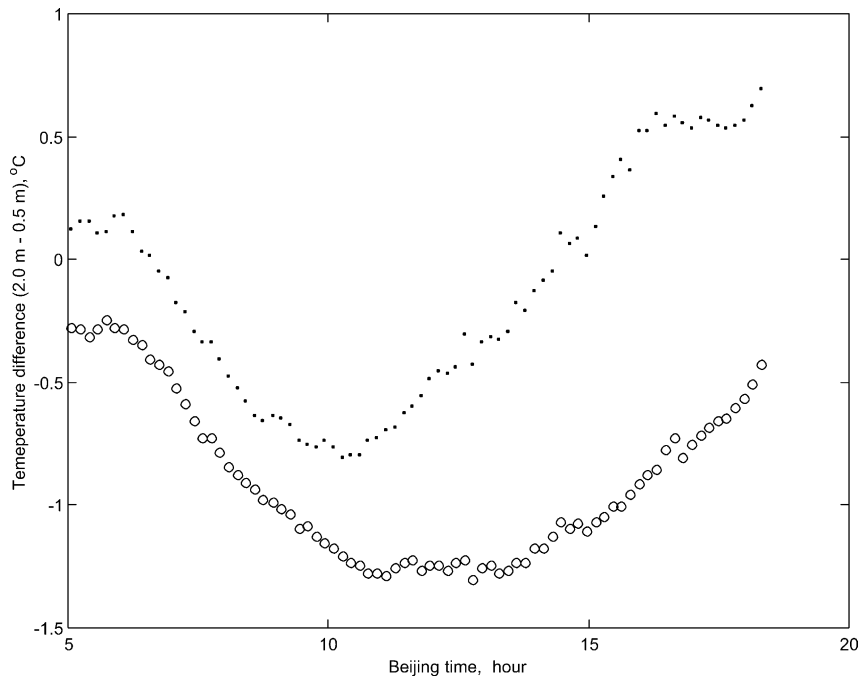


Fig. 4. Difference in dry bulb (dots) and wet bulb (circles) temperatures between the two measurements heights (26 April).

Institute of Meteorological Instruments), two soil heat flux plates (made at the Chinese Agricultural University in Beijing), and two psychrometers at heights of 0.5 and 2.0 m above the canopy. The psychrometers were made of a wet and a dry bulb precision PT100 resistance thermometer with an accuracy of  $0.05\text{ }^{\circ}\text{C}$ . They were ventilated at  $4\text{ m s}^{-1}$  and were protected by PVC radiation shields. Reversal of the two psychrometers, which occurred every 5 min, was accomplished within 15 s. Only data collected after full completion of the reversal were used to compute the temperature and humidity gradients. Field tests showed that the BREB gradient resolution was better than  $0.1\text{ }^{\circ}\text{C}$ . Fig. 4 shows a sample time series of the dry and wet bulb temperature gradients.

## 4. Experimental results

### 4.1. Background meteorological conditions

To avoid measurement errors at night due to small magnitudes of  $\lambda E$  and the humidity gradient, the fol-

lowing data analysis is limited to daylight hours (net radiation flux  $R_n > 0$ ). Relative humidity at the 2 m height was low (51–64%) despite vigorous evapotranspiration of the wheat field (Table 1). The daytime mean evapotranspiration occurred at rates faster than the equilibrium rate, with the Priestley–Taylor  $\alpha$  taking values equal to or greater than the typical value of 1.26. On 26 April, the latent heat flux exceeded the net radiation. Using a mixed-layer mass-balance model, McNaughton and Spriggs (1989) found that high  $\alpha$  values were for days with a strong capping inversion over the mixed layer.

### 4.2. Bowen ratio

Fig. 5 compares the flux Bowen ratio measured with the EC system and the gradient Bowen ratio measured with the BREB system. The flux Bowen ratio appears to be bounded by the upper limit of 0.5 which is roughly equal to the ratio  $\gamma/s$ , where  $\gamma$  is the psychrometric constant and  $s$  the slope of the saturation vapor density curve. Substituting  $\beta_f = \gamma/s$  into the

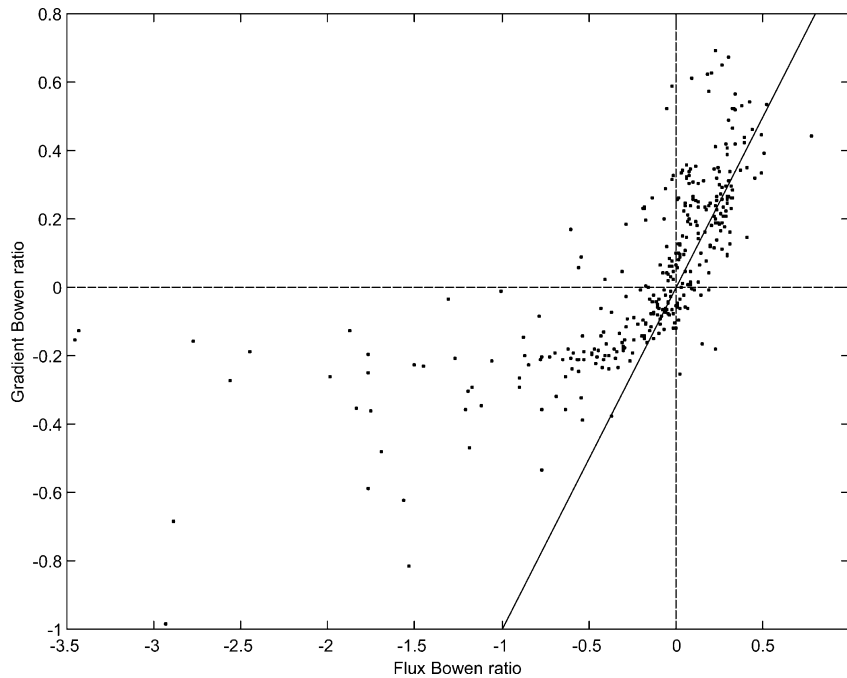


Fig. 5. A scatter plot of the gradient Bowen ratio ( $\beta_g$ ) against the flux Bowen ratio ( $\beta_f$ ). The 1:1 line is given as a reference (solid line).

#### Priestley–Taylor relationship

$$\lambda E = \alpha \frac{s}{s + \gamma} (H + \lambda E) \quad (8)$$

we obtain  $\alpha \simeq 1$ . Thus, this limit occurred at times of equilibrium ET. Chen (1985) showed that, on the assumption of  $K_H = K_W$ , dewpoint temperature and air temperature over a surface evaporating at the equilibrium rate should have the same vertical gradient, and  $\beta_g$  should also be equal to  $\gamma/s$ . Fig. 5 indicates that at the this limit,  $\beta_g$  exceeded  $\beta_f$ , or in other words, the air temperature gradient was greater than the dewpoint gradient.

During the periods with a ground-level inversion,  $\beta_f$  was much more negative than  $\beta_g$  and a large scatter was evident. On all 5 days, the surface layer was statically stable until mid-morning, became unstable for several hours, and then switched to being stable again in the afternoon. The large discrepancy between  $\beta_g$  and  $\beta_f$  was usually observed in early morning and late afternoon when the surface layer was stable. An example of this is given in Figs. 6 and 7 (see also Fig. 4).

Some of the disagreement can be explained by measurement errors. Flux loss due to inadequate instrument response at high frequencies could have affected  $H$  and  $\lambda E$  differentially. For example,  $\lambda E$  suffered from the problem of sensor separation but  $H$  did not. However, the flux loss caused by sensor separation was on the order of 10% (Lee and Black, 1994), not large enough to account for the departure of the data from the 1:1 line (Fig. 5). Another error could arise from the fact that the averaging interval might have been too short to capture the low-frequency eddy contributions to the fluxes. Over an irrigated crop, Zermeno and Hippias (1997) found that humidity variance was enhanced at low frequencies more than that of temperature, but once again the enhancement was minor in comparison to the total fluxes. It is believed that the main reason for the observed difference between  $\beta_f$  and  $\beta_g$  is inequality of the eddy diffusivities for heat and water vapor (Eq. (7)), which is discussed further.

#### 4.3. Eddy diffusivity

Following Verma et al. (1978), Fig. 8 plots the eddy diffusivities ratio as a function of the observed

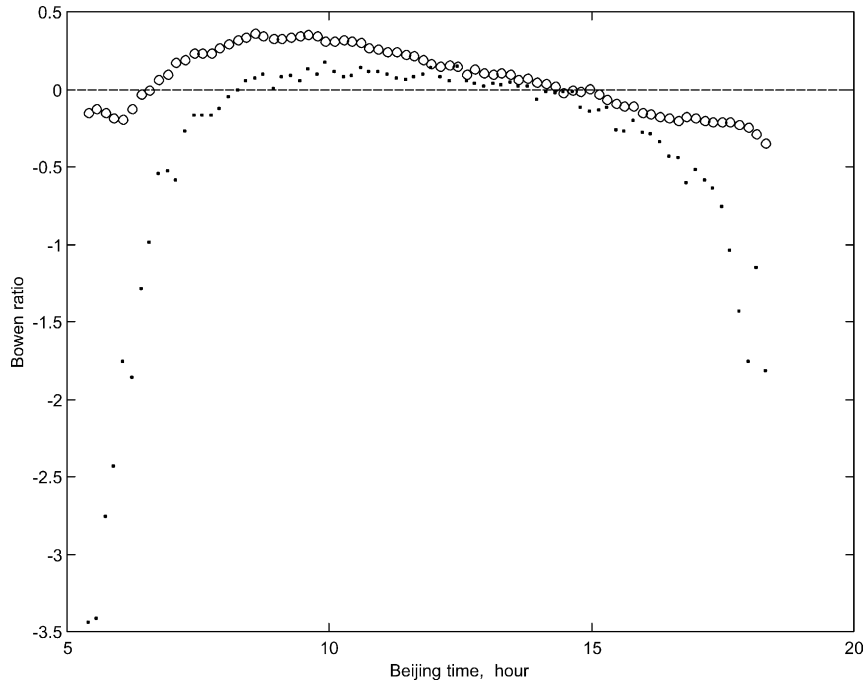


Fig. 6. Time course of the gradient (circles) and flux (dots) Bowen ratio (26 April).

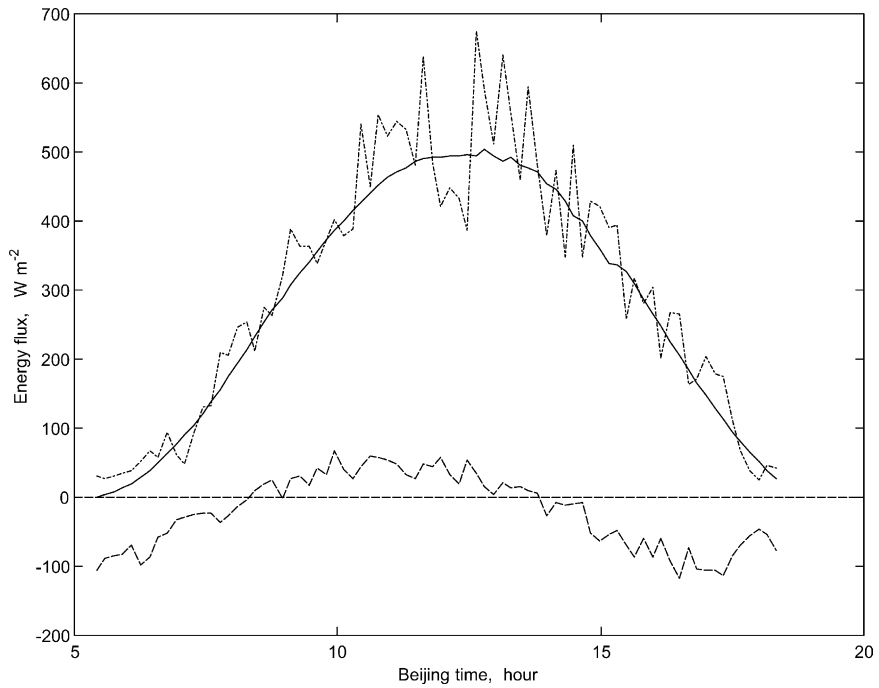


Fig. 7. Time course of the available energy flux (solid line), EC sensible heat flux (dashed line) and EC latent heat flux (dashed-dotted line) (26 April).

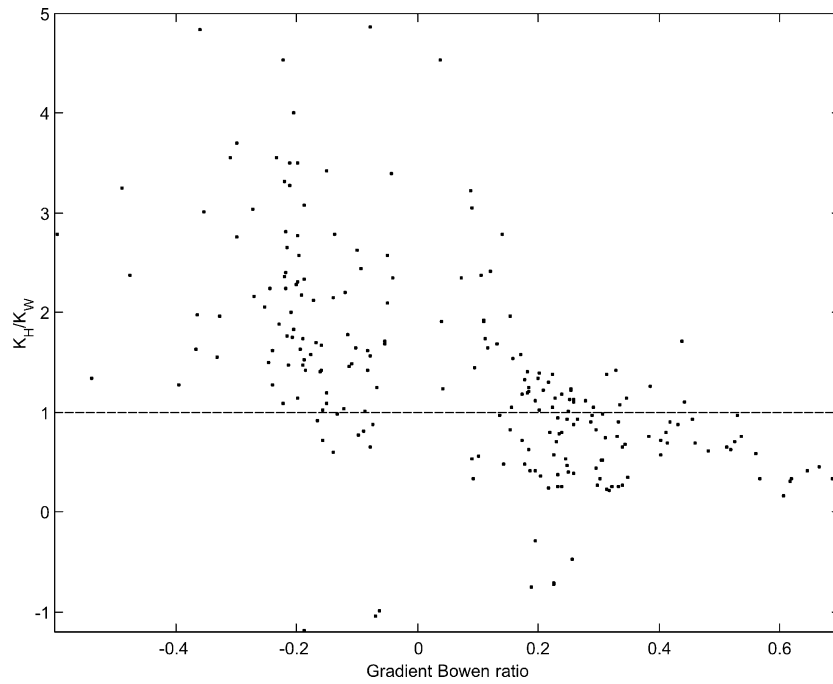


Fig. 8. The eddy diffusivities ratio plotted as a function of the gradient Bowen ratio ( $\beta_g$ ).

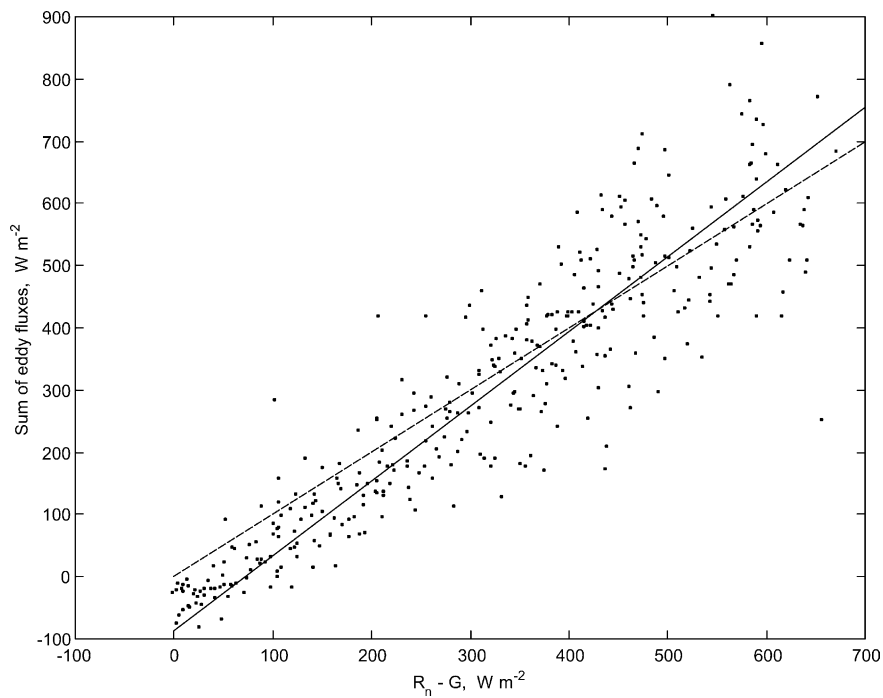


Fig. 9. A scatter plot of the total eddy fluxes  $H + \lambda E$  against the available energy flux  $R_n - G$ . Solid line represents a linear regression ( $y = -83 + 1.20x$ ,  $R^2 = 0.83$ ,  $n = 349$ ) and dashed line represents 1:1.

gradient Bowen ratio. To avoid division by small numbers, Fig. 8 uses data only if both  $H$  and  $\lambda E$  were greater than  $20 \text{ W m}^{-2}$  in magnitude and the dry and wet bulb temperature differences between the two BREB measurement heights were greater than  $0.1^\circ\text{C}$  in magnitude. About two-thirds of the observations met these data screening criteria. The median  $K_H/K_W$  ratio was 0.79 for  $\beta_g > 0$  and 2.10 for  $\beta_g < 0$ , in qualitative agreement with the theoretical analysis of the inequality problem for regional advection (Fig. 3).

The diffusivities ratio in Fig. 8 differs from Fig. 3 and/or the published studies in several important details. First, contrary to the observation by Verma et al. (1978) and the illustrative calculation in Fig. 3 which show an increasing trend of  $K_H/K_W$  as  $\beta_g$  increases, no obvious trend exists in Fig. 8 for  $\beta_g < 0$ . Second, the diffusivities ratio for  $\beta_g < 0$  is often larger than the values found in the literature (0.65–2.0). Part of the difference could be attributed to the measurement errors discussed earlier. Third, all the cited studies were performed in the surface layer with an inversion temperature profile. Fig. 8 shows that inequality of the

eddy diffusivities could also exist under convective conditions. Finally, the decreasing trend of  $K_H/K_W$  with increasing  $\beta_g$  over  $\beta_g > 0$  is in apparent disagreement with Fig. 3, but this should not be a surprise because the calculation in Fig. 3 assumes that everything else except  $\beta_g$  is a constant in Eq. (6). (The same can be said of course about the trend over  $\beta_g < 0$  in Fig. 3.)

Concern was expressed by a journal reviewer that the difference in zero-crossing time between the EC sensible heat flux (at 8:00 Beijing time, Fig. 7) and the BREB temperature gradient (at 6:00 Beijing time, Fig. 4), and the large negative sensible heat flux at near-zero  $R_n - G$  (Fig. 7), might indicate a serious instrumental problem. Certainly measurement errors were always present in any field data, but to eliminate the delay in the zero-crossing completely would require a large offset of  $0.6^\circ\text{C}$  in the temperature gradient, or an offset of  $100 \text{ W m}^{-2}$  in the sensible heat flux, neither of which we believed is likely. Alternatively, the difference in the zero-crossing could indicate a counter-gradient flux of sensible heat or a negative  $K_H$ . A negative eddy diffusivity for sensible

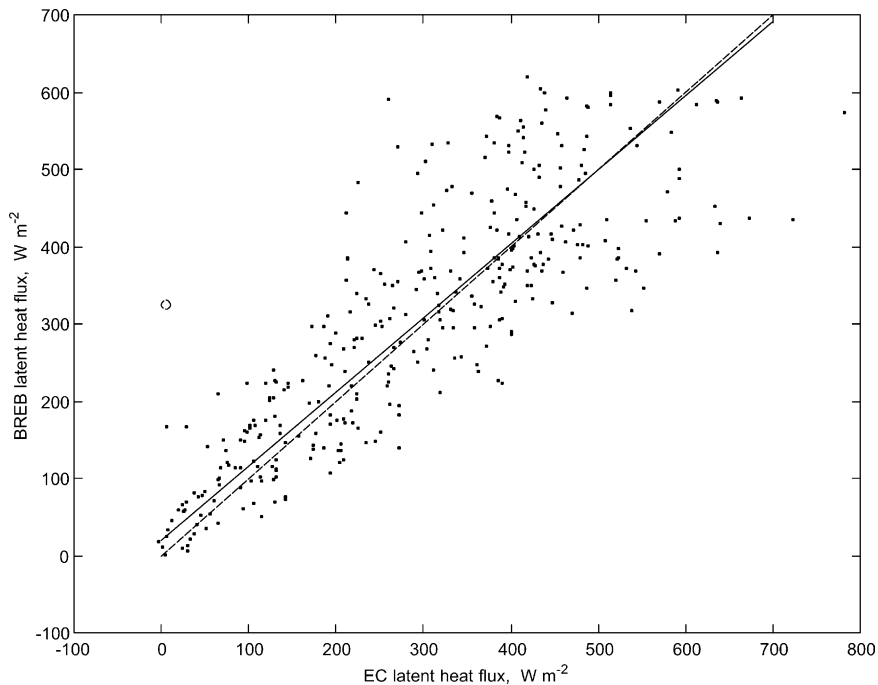


Fig. 10. A scatter plot of the latent heat flux ( $\lambda E$ ) measured with the eddy covariance against that measured with the Bowen ratio method. Solid line represents a linear regression ( $y = 19 + 0.96x$ ,  $R^2 = 0.70$ ,  $n = 340$ , excluding the outlier marked by a circle) and dashed line represents 1:1.

heat is possible if the gradient Bowen ratio is at near-zero values (e.g., in early morning hours) according to the analysis of regional advection (Fig. 3) or in local advection from wet to dry transition (Fig. 1). Negative diffusivities suggest that the simple  $K$ -theory approach is inadequate for diffusion from spatially distributed sources.

Regarding the large negative  $H$  in early morning and late afternoon hours, we are not the first to report such a phenomenon. Baldocchi (1994) observed  $H$  of about  $-50 \text{ W m}^{-2}$  at  $R_n - G = 0$  in a well-watered wheat crop. Dugas et al. (1991) reported very negative  $H$  of  $-300 \text{ W m}^{-2}$  as  $R_n - G$  approached zero in late afternoon, in an irrigated wheat field surrounded by dry soil. The negative  $H$  at times of  $R_n - G = 0$  was nearly balanced by latent heat flux in some studies (e.g., Dugas et al., 1991), but not in others (e.g., Baldocchi, 1994; Fig. 7). The lack of energy balance closure of the latter case may have been caused by a non-negligible contribution of horizontal advection to the surface layer energy balance.

In addition to regional advection, our observation may have also been influenced by local advection. Some evidence for this is given by the imperfect en-

ergy balance closure shown in Fig. 9. Because the experimental site and its neighboring farms were not irrigated at the same time, the energy fluxes of these fields might have been different. For example, if the upwind farm was extremely wet, a “wet-to-dry” transition could exist (i.e.,  $\beta_Y < 0$ ,  $\beta_g > 0$ ), making  $K_H$  smaller than  $K_W$  (Fig. 1). It is possible that diffusion from the three sources (upwind, bottom-up and top-down) may have contributed to inequality of the eddy diffusivities that is greater than observed in the dual-source diffusion, but without measurements in the neighboring farms, we cannot quantify their relative contributions to the observed fluxes.

#### 4.4. Comparison of fluxes

Fig. 9 compares the total eddy fluxes measured with the EC system,  $H + \lambda E$ , with the available energy flux,  $R_n - G$  (net radiation minus heat flux into the ground). A daytime time course of the energy balance components is given in Fig. 7. The linear regression of the data in Fig. 9 yields a slope of 1.20 and a large, negative intercept of  $-83 \text{ W m}^{-2}$ . The lack of a good energy balance could have resulted from instrument

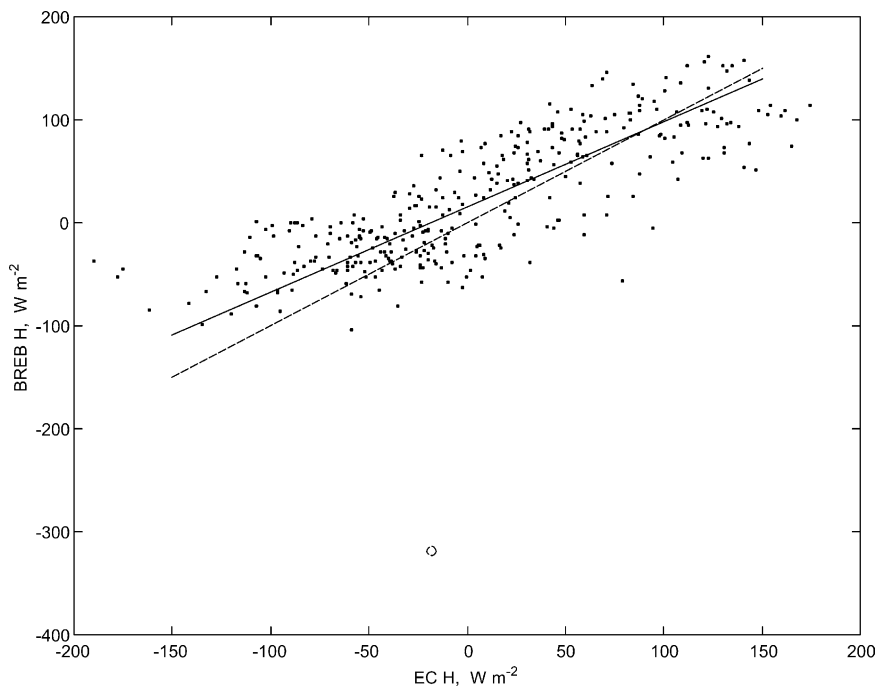


Fig. 11. Same as in Fig. 10 but for sensible heat flux (linear regression  $y = 16 + 0.83x$ ,  $R^2 = 0.64$ ,  $n = 340$ ).

biases or inadequate fetch for sensible and latent heat flux observations, although the former was unlikely because loss of fluxes due inadequate instrument response would have caused the slope of the regression to be smaller than unity.

Despite the concern about inequality of the eddy diffusivities, recent field observations show that ET with BREB is either in good agreement with the EC measurement (Rana and Katerji, 1996) or only slightly greater than the EC (Dugas et al., 1991) or lysimeter measurements (Todd et al., 2000). The sensitivity analysis of McNaughton and Laubach (1998) also shows that assuming  $K_H = K_W$ , and using BREB to calculate surface energy fluxes will usually incur minor errors. In Fig. 10, the latent heat flux measured with the BREB system is compared with that measured with EC system. Although considerable scatter is present in the data, there does not seem to be a systematic bias between the two systems. (The outlier on the lower left corner of the plot came from an observation with the  $\beta_g$  value near  $-1$  at which the BREB fluxes were undefined.) This is somewhat surprising given the large, systematic difference between the eddy diffusivities for heat and water vapor (Fig. 8). In comparison, the agreement for sensible heat flux is not as good (Fig. 11). Under stable conditions, the BREB sensible heat flux is noticeably lower in magnitude than the EC measurement.

## 5. Conclusions

On the principle of dual-source diffusion, a theoretical analysis is presented of the equality assumption involving the eddy diffusivities for sensible heat ( $K_H$ ) and water vapor ( $K_W$ ) in the surface layer. A diagnostic equation for  $K_H/K_W$  suggests that under the influence of regional advection,  $K_H/K_W > 1$  if  $\beta_g$  (the surface layer gradient Bowen ratio)  $< 0$  and  $K_H/K_W < 1$  if  $\beta_g > 0$ . The same equation is used to analyze various local advection scenarios. A similar analysis can also be performed for eddy diffusivities for trace gas fluxes.

The median values of  $K_H/K_W$ , observed over the well-watered wheat field, are 0.79 and 2.10 for periods with negative and positive  $\beta_g$ , respectively. This suggests the influence of regional advection on the measurement. Some degree of location advection might

have also be present because the experimental farm did not have adequate fetch. The experimental results and theoretical analysis show that the equality assumption is clearly inadequate in advective conditions.

Despite the concern about inequality of the eddy diffusivities, there does not seem to be a systematic bias between the ET rates measured with the BREB and the EC systems, supporting McNaughton and Laubach's (1998) sensitivity analysis showing that assuming  $K_H = K_W$ , and using BREB to calculate surface energy fluxes will usually incur minor errors. But we caution that this conclusion should not be extended to BREB measurements of fluxes of trace gases such as  $\text{CO}_2$ . This is because the sensitivity of latent heat flux to the eddy diffusivity is constrained by the available energy whereas for trace gas fluxes no equivalent constraints exist.

The two-marker argument invoked by McNaughton and Laubach (1998) is in principle no different from the top-down and bottom-up analysis of the convective boundary layer. It is not meant to rescue  $K$ -theory. On the contrary, it is an effective way to illustrate that in situations where diffusion originates from multiple sources, the simple gradient-diffusion theory does not hold. One problem arising from this is inequality of diffusivities for water vapor and sensible heat. Another problem is the negative  $K$  values (for sensible heat). Alternatively, one could use a higher-order closure model. However, Deardorff (1978) and Coppin et al. (1986) show that this is to be problematic also because of the impossibility of defining, a priori, an average vertical diffusivity which describes transport from the entire, distributed source.

## Acknowledgements

The field experiment was conducted in collaboration with Prof. Fazu Chen. This work was supported by the Chinese Academy of Sciences (CAS grant CXIOG-C00-05-02), China's Strategic Research Program in Basic Sciences (grant 2000077900) and National Natural Sciences Foundation of China (grant 49890330). The corresponding author acknowledges support by a CAS guest professorship and by the US National Science Foundation through grant ATM-0072864. We thank Drs. K.T. Paw U and S. Verma for their critical comments on this work.

## References

- Baldocchi, D., 1994. A comparative study of mass and energy exchange over a closed C3 (wheat) and an open C4 (corn) canopy. I. The partitioning of available energy into latent and sensible heat exchange. *Agric. For. Meteorol.* 67, 193–220.
- Barr, A.B., Betts, A.K., 1997. Radiosonde boundary layer budgets above a boreal forest. *J. Geophys. Res.* 102, 29205–29212.
- Blad, B.L., Rosenberg, N.J., 1974. Lysimetric calibration of the Bowen ratio–energy balance method for evapotranspiration estimation in the central Great Plains. *J. Appl. Meteorol.* 13, 227–236.
- Betts, A.K., Desjardins, R.L., MacPherson, J.I., 1992. Budget analysis of the boundary layer grid flights during FIFE 1987. *J. Geophys. Res.* 97, 18533–18546.
- Brunet, Y., Itier, B., McAneney, J., Lagouarde, P.J., 1994. Downwind evolution of scalar fluxes and surface resistance under conditions of local advection. Part II. Measurements over barley. *Agric. For. Meteorol.* 71, 227–245.
- Chen, J., 1985. A graphical extrapolation method to determine canopy resistance from measured temperature and humidity profiles above a crop canopy. *Agric. For. Meteorol.* 33, 291–297.
- Coppin, P.A., Raupach, M.R., Legg, B.J., 1986. Experiments on scalar dispersion within a model plant canopy. Part II. An elevated plane source. *Bound. Layer Meteorol.* 35, 167–191.
- Deardorff, J.W., 1978. Closure of second- and third-moment rate equations for diffusion in homogeneous turbulence. *Phys. Fluids* 21, 525–530.
- Denmead, O.T., Bradley, E.F., 1985. Flux–gradient relationships in a forest canopy. In: Hutchinson, B.A., Hicks, B.B. (Eds.), *The Forest–Atmosphere Interactions*. Reidel, pp. 421–442.
- Dugas, W.A., Heuer, M.L., Mayeux, H.S., 1999. Carbon dioxide fluxes over bermudagrass, native prairie, and sorghum. *Agric. For. Meteorol.* 93, 121–139.
- Dugas, W.A., Fritschen, L.J., Gay, L.W., Held, A.A., Matthias, A.D., Reicosky, D.C., Steduto, P., Steiner, J.L., 1991. Bowen-ratio, eddy-correlation, and portable chamber measurements of sensible and latent heat flux over irrigated spring wheat. *Agric. For. Meteorol.* 56, 1–20.
- Godtstein, A.H., Fan, S.M., Goulden, M.L., Munger, J.W., Wofsy, S.C., 1996. Emissions of ethene, propene, and 1-butene by a midlatitude forest. *J. Geophys. Res.* 101, 9149–9157.
- Jones, H.G., 1992. *Plants and Microclimate: A Quantitative Approach to Environmental Plant Physiology*, 2nd ed. Cambridge University Press, New York.
- Kroon, L.J.M., de Bruin, H.A.R., 1995. The Crau field experiment: turbulent exchange in the surface layer under conditions of strong local advection. *J. Hydrol.* 166, 327–352.
- Lang, A.R.G., McNaughton, K.G., Chen, F., Bradley, E.F., Ohaki, E., 1983. Inequality of eddy transfer coefficients for vertical transport of sensible and latent heats during advective inversions. *Bound. Layer Meteorol.* 25, 25–41.
- Laubach, J., McNaughton, K.G., Wilson, J.D., 2000. Heat and water vapour diffusivities near the base of a disturbed stable internal boundary layer. *Bound. Layer Meteorol.* 94, 23–63.
- Launder, B.E., 1978. Heat and mass transport. In: Bradshwa, P. (Ed.), *Turbulence*, 2nd ed. Springer-Verlag, New York, pp. 231–287.
- Lee, X., Black, T.A., 1994. Relating eddy correlation sensible heat flux to horizontal sensor separation in the unstable surface layer. *J. Geophys. Res.* 99, 18545–18553.
- Leuning, R., Dunin, F.X., Wang, Y.-P., 1998. A two-leaf model for canopy conductance, photosynthesis and partitioning of available energy. II. Comparison with measurements. *Agric. For. Meteorol.* 91, 113–125.
- McNaughton, K.G., Laubach, J., 1998. Unsteadiness as a cause of non-equality of eddy diffusivities for heat and vapour at the base of an advective inversion. *Bound. Layer Meteorol.* 88, 479–504.
- McNaughton, K.G., Spriggs, T.W., 1989. An evaluation of the Priestley and Taylor equation and the complementary relationship using results from a mixed-layer model of the convective boundary layer. In: Black, T.A., Spittlehouse, D.L., Novak, M.D., Price, D.T. (Eds.), *Estimation of Areal Evapotranspiration*. IAHS Publication no. 177, pp. 89–104.
- Meyers, T.P., Hall, M.E., Lindberg, S.E., Kim, K., 1996. Use of the modified Bowen-ratio technique to measure fluxes of trace gases. *Atmos. Environ.* 30, 3321–3329.
- Moeng, C.-H., Wyngaard, J.C., 1984. Statistics of conservative scalars in the convective boundary layer. *J. Atmos. Sci.* 41, 3161–3169.
- Motha, R.P., Verma, S.B., Rosenberg, N.J., 1979. Exchange coefficients under sensible heat advection determined by eddy correlation. *Agric. Meteorol.* 20, 273–280.
- Price, T.D., Black, T.A., 1991. Effects of summertime changes in weather and root-zone soil water storage on canopy CO<sub>2</sub> flux and evapotranspiration of two juvenile Douglas-fir stands. *Agric. For. Meteorol.* 53, 303–323.
- Rosenberg, N.J., Blad, B.L., Verma, S.B., 1983. *Microclimate: The Biological Environment*, 2nd ed. Wiley, New York.
- Rana, G., Katerji, N., 1996. Evapotranspiration measurement for tall plant canopies: the sweet sorghum case. *Theor. Appl. Climatol.* 54, 187–200.
- Todd, R.W., Evett, S.R., Howell, T.A., 2000. The Bowen ratio–energy balance method for estimating latent heat flux of irrigated alfalfa evaluated in a semi-arid, advective environment. *Agric. For. Meteorol.* 103, 335–348.
- Verma, S.B., Rosenberg, N.J., Blad, B.L., 1978. Turbulent exchange coefficients for sensible heat and water vapor under advective conditions. *J. Appl. Meteorol.* 17, 330–338.
- Wyngaard, J.C., Brost, R.A., 1984. Top-down and bottom-up diffusion of a scalar in the convective boundary layer. *J. Atmos. Sci.* 41, 102–112.
- Zermeno, A., Hipps, L.E., 1997. Downwind evolution of surface fluxes over a vegetated surface during local advection of heat and saturation deficit. *J. Hydrol.* 192, 189–210.